Permanent Trapping of CO_2 in Single-Walled Carbon Nanotubes Synthesized by the HiPco Process

Christopher Matranga* and Bradley Bockrath

National Energy Technology Laboratory, United States Department of Energy, P.O. Box 10940, Pittsburgh, Pennsylvania 15236

Infrared spectroscopy is used to study trapped and physisorbed CO_2 in single-walled carbon nanotube bundles (SWNTs) synthesized by the HiPco process. CO_2 is entrapped within the SWNTs by acid oxidation of the unpurified sample followed by vacuum heating to 700 K. The trapped CO_2 has a single ν_3 mode at 2327 cm^{-1}, is stable during temperature cycling from 77 to 700 K, and remains after venting to room air. CO_2 physisorption studies show a ν_3 mode at 2330 cm^{-1} for the as-received HiPco samples, 2340 cm^{-1} for the acid-oxidized sample, and 2327 and 2340 cm^{-1} for the oxidized sample after vacuum heating. The sites responsible for the infrared peaks of the physisorbed and trapped species are discussed.

Introduction

Previously, we have reported on how oxygen-containing functionalities on acid-oxidized single-walled carbon nanotube bundles (SWNTs) synthesized by laser ablation can generate CO_2, which becomes permanently trapped within the nanotube bundle.[1] This trapped CO_2 is stable in a vacuum from 5 to 700 K, remains after venting to ambient conditions, and persists for time scales of at least 2 months in samples studied under vacuum.[1] The entrapment of this CO_2 likely involves the rearrangement of functionalities at defect sites as they decompose, which locks the generated CO_2 into sites inside the nanotubes themselves as well as the spaces between nanotubes in the bundle. Rearrangements of the bundle itself due to the annealing effect of vacuum heating might also play a role.

Vacuum heating is a standard processing technique for SWNTs, so recognizing and understanding the trapped CO_2 occurring from this is an important step in using these materials as sensors, gas storage materials, and separation membranes. In fact, studying the confined CO_2 in these materials could be fruitful for our general understanding of molecular behavior in low-dimensional systems. Techniques to separate bundles and manipulate individual nanotubes are rapidly being mastered,[2−4] so the controlled ability to trap different molecules in SWNTs with their eventual release could possibly be exploited as a nanometer-scale storage and delivery system.

In this work, we report infrared spectroscopic studies of SWNTs prepared by the HiPco process before and after acid oxidation. We find that acid-oxidized HiPco samples are capable of generating permanently trapped CO_2, much like oxidized SWNTs prepared by laser ablation,[1] and the behavior of trapped and physiorbed CO_2 in these materials displays many similarities. This work shows that the entrapment of CO_2 during the vacuum heating of acid-oxidized SWNTs seems to be a general process that is not limited to tubes of a particular size distribution, synthetic procedure, type of residual metal catalyst, or solvent used to cast the thin films for IR analysis. Furthermore, by studying gas adsorption in SWNTs prepared by different synthetic procedures we are starting to recognize more general properties of gas interactions with these materials that will likely be of broader scientific interest.

In this paper, we employ descriptions commonly used in the literature for the available adsorption sites on a nanotube bundle.[5−7] These sites are (i) the space inside nanotubes of the bundle (endohedral sites), (ii) the space between individual nanotubes (interstitial sites), and (iii) the "groove" formed where the curved outer surfaces of individual tubes meet on the most external periphery of the bundle (groove sites). Clearly, the possibility exists for other "sites" like those associated with the three-stripe phase or other types of multilayer adsorption.[5] We do not expect to encounter these types of sites since they are associated with higher coverages.

Experimental Section

Samples made by the HiPco process were obtained as unpurified solid material from Carbon Nanotechnologies Incorporated and are reported to have average diameters of approximately 1.1 nm with sample purities of SWNT carbon that are greater than 90 atomic percent.[8] From thermogravimetric analysis (TGA), we find that this material has ∼18 wt % (grams Fe/grams of sample) of residual Fe catalyst, which is in agreement with earlier reports.[8] The unpurified HiPco nanotubes were later dispersed in toluene so thin films could be made for IR analysis.

Acid-oxidized HiPco samples were prepared by refluxing the unpurified material in 3 M HNO_3 for 8 h, the sample was then allowed to sit unheated in this solution overnight, and an additional 8 h reflux was performed the next day. The refluxed sample was filtered and rinsed with Ultrapure water until the rinse was pH neutral. The still damp sample was dispersed in acetone so thin films could be made for IR analysis. We find that if the samples are allowed to dry before dispersing in acetone, a "Bucky Paper" is formed, which is difficult to redisperse in solvent. TGA analysis shows that the residual Fe content of the acid-refluxed nanotubes has been reduced to ∼3 wt %.

Infrared studies were taken in the transmission geometry with the samples housed in a stainless steel vacuum chamber

* Corresponding author. Phone: 412-386-4114. Fax: 412-386-5920. E-mail: matranga@netl.doe.gov.

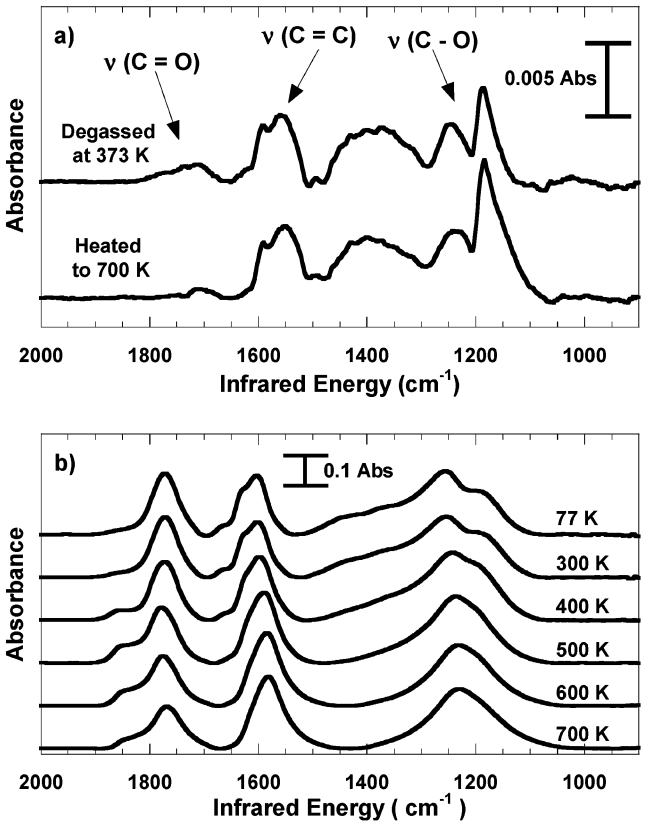

Figure 1. IR spectra of the oxygen-containing functionality region. (a) As-received HiPco sample measured at 77 K after degassing at 373 K (top spectrum) and at 77 K after heating to 700 K (bottom spectrum). Data are intentionally offset on the *y* axis for clarity. Only minor changes are created in the carbonyl bands by heating to 700 K. (b) Acid-refluxed HiPco nanotubes during vacuum heating. The temperature listed in the legend for each spectrum in (b) is the temperature of the sample when the measurement was conducted.

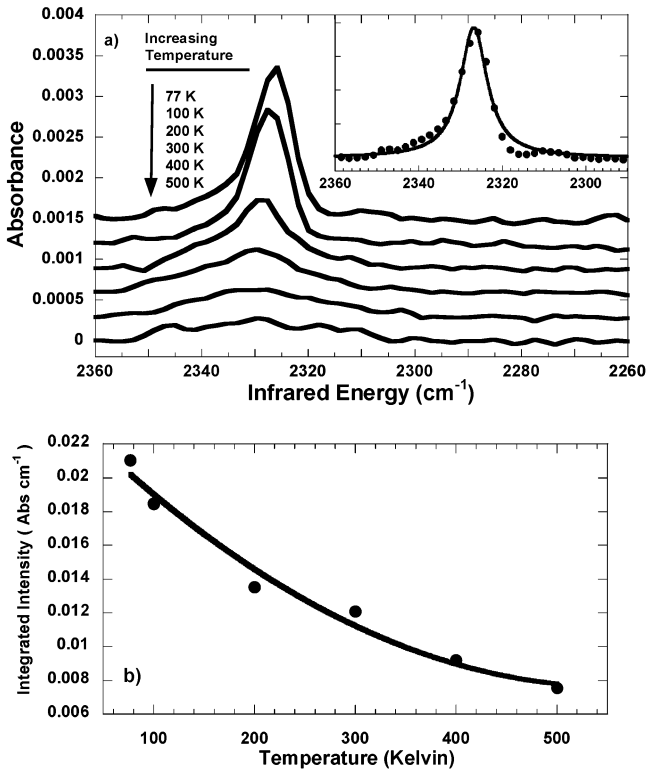

Figure 2. IR data for the trapped CO_2 species. (a) Bandwidth and intensity variations of the trapped ν_3 mode with measurement temperature. Data are intentionally offset on the *y* axis for clarity. The inset shows the spectrum at 77 K fitted to a simple Lorentzian line shape, yielding a resonance frequency of 2327 cm^{-1} and a fwhm of 8 cm^{-1}. (b) Integrated intensity for the data in (a) determined numerically. The solid line is meant as a guide to the eye.

described previously.[1] Infrared samples were thin films prepared by dispersing the sample directly on a plane parallel CaF_2 window (Janos Technology) and evaporating the solvent in a 120 °C oven for ∼5 min.[1] The thickness of the film was adjusted to give a nonresonant background absorption of ∼1.0 OD at 2300 cm^{-1}, which gave enough sample thickness for us to observe CO_2 entrapment and physisorption. Samples were degassed in the vacuum chamber at 373 K for 2 h prior to use. Preliminary work comparing degassed samples to ones used without degassing indicates that no differences exist. Since the plane parallel window has a negligibly low surface area compared to the SWNT sample, we see no artifacts from CO_2 adsorption on the window during physisorption studies, and the background subtraction is therefore very complete.

Results and Discussion

Oxygen Functionalities and Vacuum Heating. The changes of oxygen-containing functionalities are shown by the IR spectra in Figure 1. The as-received HiPco samples (Figure 1a) show carbonyl peaks (∼1710−1780 cm^{-1}), C═C vibrations (∼1550−1600 cm^{-1}), and C−O bands (∼1180−1250 cm^{-1}). Vacuum heating of the sample to 700 K does not create any significant changes in the IR spectra in this region, suggesting that the moderate degree of functionality seen is a stable modification to defect sites in the nanotube structure.

Acid refluxing of the sample (Figure 1b) drastically increases the intensity of the carbonyl bands with a strong peak at ∼1770 cm^{-1} and a weaker shoulder at ∼1850 cm^{-1}. The C═C and C−O bands also increase in intensity. The increased integrated intensity of all these bands cannot be accounted for by the relative changes in film thickness occurring for different experimental runs and must be related to a higher density of functionalities in the acid-refluxed samples.

Vacuum heating of the refluxed sample creates an intensity increase in the high-energy shoulder (∼1850 cm^{-1}) of the carbonyl band with an associated intensity decrease with the larger 1770 cm^{-1} peak. The higher energy bands associated with C═C functionalities decrease in intensity, and a single band evolves at ∼1580 cm^{-1}, which is close in energy to what is typically associated with the IR active phonon in various graphitic carbons.[9−13] Heating to 700 K causes the C−O bands to form a single band at ∼1230 cm^{-1}.

There are some differences in the results from vacuum heating of the acid-refluxed HiPco samples and acid-oxidized SWNTs made by laser ablation. In particular, heating of the acid-refluxed HiPco sample does not result in the drastic decomposition and frequency shifting of carbonyl functionalities seen in the SWNTs prepared by ablation.[1,12,14,15] Even the initial vacuum heating of the HiPco samples before acid treatment (Figure 1a) did not create significant changes in the IR spectra. This result hints at the relative stability of the oxygen-containing functionalities on the HiPco samples in the same temperature range where functionalities on the SWNTs made by ablation show significant decomposition.[1,12,14,15]

Trapped CO_2. The refluxed HiPco sample was heated to 700 K in a manner analogous to that used to generate trapped CO_2 in oxidized nanotubes made from laser ablation.[1] In the present case, evidence for a trapped CO_2 species is again clearly seen in the IR spectra.[1] At 77 K (Figure 2a) the IR spectrum is

well described by a Lorentzian line shape centered at ~2327 cm^{-1} with a fwhm of ~8 cm^{-1}, suggesting that CO_2 is trapped in a single type of environment. This differs somewhat from the laser-ablated nanotubes that gave peaks at ~2330 and 2340 cm^{-1}, which were tentatively assigned to CO_2 trapped in endohedral and interstitial sites, respectively.[1] On the basis of the single trapped peak at ~2327 cm^{-1}, previous work,[1,16] and CO_2 physisorption studies on these samples (see below), we argue that the peak at 2327 cm^{-1} is likely the result of endohedrally trapped CO_2 with the interstitial spaces being unoccupied. The closer packing of the bundle caused by the smaller tube diameters in the HiPco samples should make the interstitial sites smaller and therefore less accessible.

Figure 2 shows the behavior for the ν_3 mode of the trapped CO_2 as a function of temperature. As the sample is heated, the ν_3 band decreases in intensity and broadens. Above 500 K, the trapped species becomes difficult to detect. As the sample is subsequently cycled from 77 to 500 K, the intensity variations seen in Figure 2 are reproducible for each given temperature. Regeneration of the original spectrum on cooling demonstrates that none of the trapped gas is lost. The broadening and intensity loss seen in Figure 2 is nearly the same as what was observed for the laser-ablated nanotubes.[1] No new CO_2 is introduced into the chamber, so these variations result from a physical process involving the trapped CO_2 and not from the loss and regeneration of the trapped species. Figure 2b shows that the integrated intensity decreases by a factor of 3 during heating from 77 to 500 K. If changes in the dynamic dipole moment, $(\partial\mu/\partial Q_i)$, are responsible for these intensity variations, this indicates a $\sqrt{3}$ decrease for $(\partial\mu/\partial Q_i)$ of the ν_3 mode.[17,18]

The integrated intensity of the ν_3 band at 77 K in Figure 2 is almost a factor of 10 smaller than previously observed for laser-ablated nanotubes.[1] This difference cannot easily be accounted for by simple variations in sample-to-sample film thickness and suggests that the density of trapped CO_2 in oxidized HiPco nanotubes is lower. This lower density is likely related to the relatively minor decomposition seen for the oxygen functionalities in Figure 1b, which in turn would generate less CO_2 for entrapment.

Venting of the sample to room air at 300 K creates no significant changes in the IR spectrum of the oxygen functionalities and does not cause the release of the trapped CO_2 species (Figure 3a). Raman analysis of the as-received, acid-refluxed (before vacuum heating), and acid-refluxed (after vacuum heating and venting) samples are displayed in Figure 3b. Acid refluxing causes changes in the relative intensities of the radial breathing modes (RBMs), particularly of the modes at 270, 188, and 172 cm^{-1}. Vacuum heating of the refluxed sample does not return the relative intensity of the RBMs to their initial values. The Raman changes for the RBMs suggest that the oxidative refluxing process is shifting the diameter distribution toward larger values, as suggested for other oxidative procedures.[19−21] We urge caution with this interpretation since one might expect the extensive functionalization on these samples to change relative Raman cross sections through perturbation of the electronic density of states. The samples of Figure 3b are only probed with a 532 nm source to illustrate the relative intactness of the SWNTs, and a more complete UV/vis/NIR, Raman, or TEM analysis[4,22−24] would be necessary to be definitive about shifting diameter distributions.

Associated with the changes in the RBMs are increases in the relative intensity of the D band near 1330 cm^{-1} after refluxing with a subsequent decrease after vacuum heating. These changes are easily explained by defects created in the

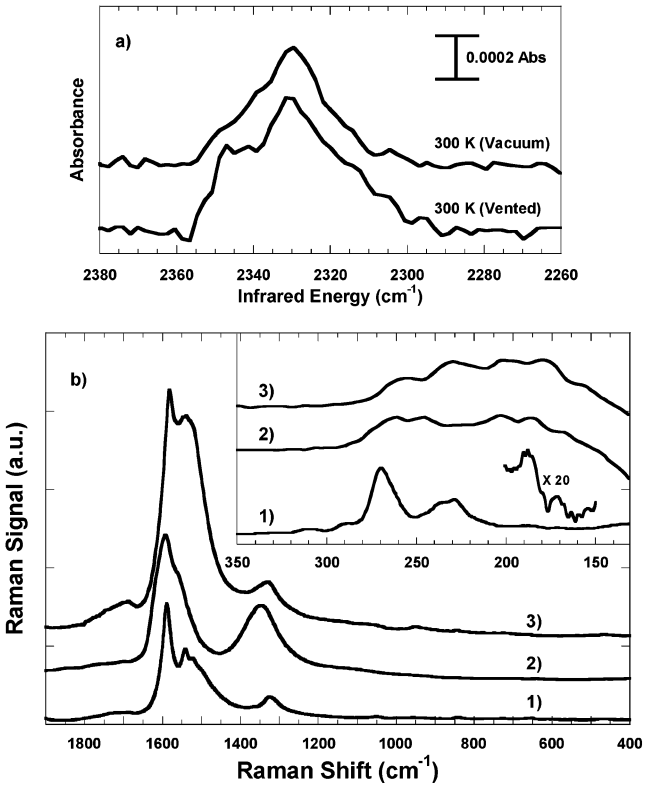

Figure 3. Vibrational spectra of the HiPco samples. (a) IR spectra of the trapped CO_2 species before and after venting to room air. The ν_3 band remains, indicating that the trapped CO_2 species is not released by exposure to ambient conditions. (b) Raman spectra of the (1) as-received HiPco, (2) acid-oxidized HiPco, and (3) acid-oxidized and vacuum-heated HiPco sample. Raman spectra were collected with a 532 nm excitation of the thin film samples used in the IR experiments with 1 and 2 being collected before the samples were introduced into the vacuum system for IR studies and 3 being collected from the same sample displayed in (a) after vacuum heating followed by venting to room air. The inset shows an enlargement of the spectral region where the RBMs occur.

sp^2 network of the nanotube sidewalls by functionalities that are partially removed by the later vacuum heating step. Also noted is the structure in the G bands (~1400−1650 cm^{-1}) that occurs from the tangential modes of nanotubes with differing chirality. This G band structure undergoes broadening and shifting during the acid-refluxing and vacuum-heating steps but is always present, indicating the structure of the SWNTs has not been completely disrupted.

Physisorption of Gas Phase CO_2. The physisorption of gas phase CO_2 before and after various processing steps was used to gain an understanding of how adsorption sites change with oxidation and heating steps. The results show that chemical functionalization blocks access to certain adsorption sites, and previous work interpreted this effect to be a result of blocked access to interior sites on the bundle.[15,25−27] Figure 4a shows IR spectra of CO_2 physisorbed on the as-received HiPco sample. A peak is seen at ~2330 cm^{-1}, which grows in intensity with increasing pressure. This peak is similar in frequency to what has been observed for physisorbed[1,16] and trapped[1] species in previous work, where it was assigned to CO_2 in endohedral sites. This IR peak is also close in energy to the 2327 cm^{-1} peak observed for the trapped species in Figure 2a. Most of the intensity for the IR spectra at the highest CO_2 pressure of 0.00038 mTorr comes from a peak at 2329 cm^{-1}, but about a fourth of the integrated intensity can be accounted for by a second peak at 2337 cm^{-1}. This suggests that other adsorption

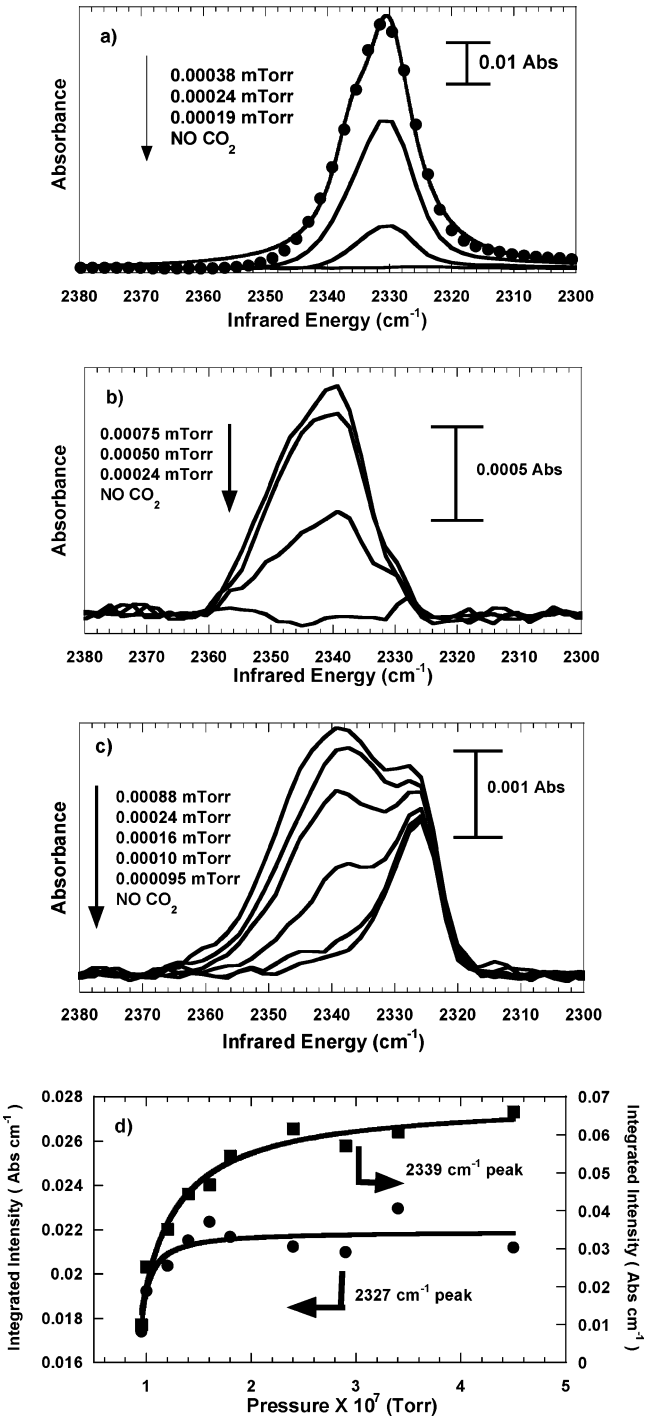

Figure 4. IR data for physisorbed CO_2 at 77 K. (a) Results for the as-received HiPco nanotubes. The solid dots for the 0.00038 mTorr spectra are experimental data points, and the solid line through these points is a 2 Lorentzian fit (see text). The other spectra in (a) are represented by solid lines. Pressures indicated are static pressures of CO_2 in the cell when the measurement was taken. (b) IR spectra for physisorbed CO_2 on the acid-refluxed HiPco nanotubes. (c) IR for CO_2 physisorption on the refluxed and vacuum-heated HiPco samples. There is intensity from trapped CO_2 before any gas phase CO_2 is introduced to the vacuum chamber. (d) Integrated intensity of the deconvoluted bands at 2339 and 2327 cm^{-1} using the data from (c). The different *y* axis scales for the two data sets in (d) were used to illustrate saturation of the integrated intensity with increasing CO_2 pressure.

sites are accessed at higher coverages with their IR peaks being convoluted with the main peak near 2330 cm^{-1} (see discussion below).

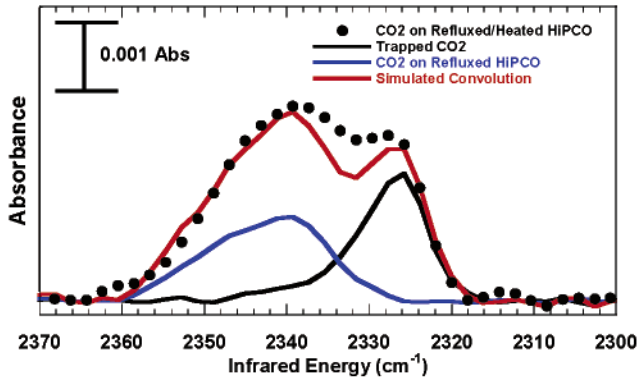

Figure 5. Spectra illustrating how the IR peaks for the physisorbed CO_2 on the refluxed/heated SWNTs (solid dots) can be constructed from spectra for trapped CO_2 (black line) and from those for CO_2 physisorbed on the refluxed sample before heating (blue line). The two-component spectra were multiplied by an arbitrary scaling factor and then added to form the convolution of these spectra (red line).

The result of one primary peak at 2330 cm^{-1} in the IR spectra of Figure 4a suggests that CO_2 physisorbs in endohedral sites in the as-received HiPco sample. Endohedral adsorption requires nanotubes with open ends or a significant amount of holes in the side wall. A previous micropore study has found evidence that as-received HiPco nanotubes are fairly open for endohedral adsorption.[27] Our results seem to agree with this finding.

Figure 4b shows IR spectra of CO_2 physisorption on the acid-refluxed HiPco sample. The oxygen functionalities introduced by the refluxing process should decorate side wall defects and the open ends of the nanotubes and thus hinder access to endohedral and interstitial sites on the bundles. The IR spectra in Figure 4b show one single peak at ~2340 cm^{-1}, which is very similar in frequency to previous IR spectra reported for both physisorbed and trapped CO_2 in the acid-oxidized SWNTs made by ablation.[1] In the previous work, we have assigned the peak near 2340 cm^{-1} on the functionalized samples to groove site adsorption.

Figure 4c shows the physisorption of CO_2 on the acid-refluxed HiPco sample after heating to 700 K. The trapped species at 2327 cm^{-1} is apparent before gas phase CO_2 is introduced to the cell. The addition of CO_2 causes an increase in the integrated intensity of the band at 2339 cm^{-1} as well as the peak at 2327 cm^{-1}. Deconvolution of the bands with a 2 Lorentzian line shape (Figure 4d) shows a ~20% intensity increase of the 2327 cm^{-1} peak before saturation and a ~80% increase in the 2339 cm^{-1} peak. The slight intensity growth for the 2327 cm^{-1} peak suggests that the vacuum heating reopens the oxidized tubes, allowing gas phase CO_2 access to a portion of the endohedral sites associated with creating this IR peak.[1,16]

One key finding from the current work is there is no strong evidence for interstitial trapping or physisorption as previously seen for various gases in other studies.[1,27–29] We find the 2340 cm^{-1} peak from physisorbed CO_2 on the oxidized HiPco samples, yet heating does not create the trapped species near this frequency previously associated with interstitial trapping,[1] suggesting these sites are less accessible in the HiPco bundles. This makes it difficult to attribute the growth of the 2340 cm^{-1} shoulder in Figure 4c to interstitial physisorption in bundles partially opened by vacuum heating, as suggested previously.[1] To illustrate this concept, we convolute spectra for the trapped CO_2 species (presumably endohedral CO_2) and physisorbed CO_2 species on the acid-refluxed sample (presumably groove site CO_2) and compare them with spectra for physisorbed CO_2 on the refluxed/heated HiPco sample (Figure 5). The IR spectrum

for the refluxed/heated sample is well represented by this simple simulation, suggesting that the 2340 cm^{-1} species in Figure 4c is indeed the result of the same species we see in Figure 4b. Although having similar frequencies, the 2340 cm^{-1} bands seen with CO_2 physisorption on oxidized SWNTs before and after vacuum heating in previous work[1] have very different morphologies and bandwidths, much unlike what we see in Figure 5a. We feel this suggests that interstitial sites of the laser-ablated nanotubes are accessed and those of the HiPco nanotubes are not.

Another factor that must be addressed is what appears to be a single peak at 2330 cm^{-1} for the as-received HiPco nanotubes in Figure 4a, which we believe to be related to endohedral adsorption. When these endohedral sites are blocked through functionalization (Figure 4b), a peak at 2340 cm^{-1} results from CO_2 physisorption which likely is not related to endohedral sites and instead must be CO_2 in groove sites. Figures 4a and 4b indicate that both groove and endohedral sites are accessible at the temperature and pressures used in this experiment. For the case of the as-received HiPco nanotubes, where neither site is blocked by functionalization, evidence for both species should be seen in the IR spectra at higher coverages. As discussed above, the higher coverage IR spectra in Figure 4a can be accounted for by a 2 Lorentzian line shape with peaks at 2330 and 2337 cm^{-1} having an integrated intensity ratio of 4 to 1, respectively. This seems to indicate that both the endohedral and groove sites are being populated, although it does not have the edifying spectroscopic signature of two well-resolved IR peaks.

The experimental evidence that groove and larger interstitial spaces yield similar vibrational frequencies for CO_2 is a complicating factor in analyzing these spectra.[1,16] At certain pressures one would expect all sites to be occupied in a fully open bundle, with large interstitial spaces meaning the IR spectra for groove and interstitial sites would definitely be difficult to separate. The different adsorption energetics associated with these sites should allow us to selectively fill or displace these sites by conducting experiments at different temperatures and coverages. Xe displacement has been shown to selectively displace molecules, and it easily displaced the 2330 cm^{-1} peak and possibly the 2340 cm^{-1} in other CO_2 studies.[16,25,26] We are currently working on detailed computational and experimental studies involving Xe displacement, which should help resolve some of the issues complicating IR spectra of CO_2 adsorbed in groove and interstitial spaces.

Despite some complications, we are starting to see some very general results for CO_2 interactions with SWNTs: (i) CO_2 can become entrapped by heating acid-oxidized SWNTs; (ii) the ν_3 frequency of the entrapped species occurs near 2330 cm^{-1} in current and previous work, and a second trapped species at 2340 cm^{-1} has been observed with nanotubes made by laser ablation[1]; (iii) physisorbed CO_2 on acid-oxidized SWNTs creates an IR band at 2340 cm^{-1}; (iv) the intensity and bandwidth of the ν_3 mode of the trapped CO_2 species have a strong temperature dependence.

In addition, the current work shows us (i) the as-received HiPco samples appear to physisorb CO_2 in endohedral sites, suggesting they are relatively open, and (ii) the naturally occurring oxygen functionalities on the as-received HiPco samples are fairly stable up to 700 K, as are functionalities introduced by the acid-refluxing step.

Summary

Acid-oxidized HiPco SWNTs produce permanently trapped CO_2 when vacuum heated. The generation of this trapped species in HiPco SWNTs and its previous observation in other SWNTs show that the entrapment of CO_2 during the vacuum heating of functionalized nanotubes is a more general process not limited to samples of particular size distribution, impurity content, or synthetic origin. The entrapped species in the HiPco sample is believed to be locked in endohedral sites, with interstitial sites being unoccupied. Physisorption studies also suggest that interstitial sites in HiPco samples are not accessible to CO_2.

Acknowledgment. We thank Milton Smith, Ed Bittner, Liang Chen, Karl Johnson, and Shelia Hedges for useful discussions. We thank Oleg Byl, Peter Kondratyuk, Wai-Leung Yim, and John Yates for sharing their results for CO_2 adsorption on nanotubes prior to publication. Reference in this work to any specific commercial product is to facilitate understanding and does not necessarily imply endorsement by the United States Department of Energy.

References and Notes

(1) Matranga, C.; Chen, L.; Smith, M.; Bittner, E.; Johnson, J. K.; Bockrath, B. *J. Phys. Chem. B* **2003**, *107*, 12930.
(2) Tour, J.; Dyke, C. *Nano Lett.* **2003**, *3*, 1215.
(3) Strano, M. *J. Am. Chem. Soc.* **2003**, *125*, 16148.
(4) O'Connell, M.; Bachilo, S.; Huffman, C.; Moore, V.; Strano, M.; Haroz, E.; Rialon, K.; Boul, P.; Noon, W.; Kittrell, C.; Ma, J.; Hauge, R.; Weisman, R. B.; Smalley, R. E. *Science* **2002**, *297*, 593.
(5) Calbi, M. M.; Cole, M. W. *Rev. Mod. Phys.* **2001**, *73*, 857.
(6) Zambano, A. Z.; Talapatra, S.; Migone, A. D. *Phys. Rev. B* **2001**, *64*, 75415.
(7) Stan, G.; Bojan, M. J.; Curtarolo, S.; Gatica, S. M.; Cole, M. W. *Phys. Rev. B* **2000**, *62*, 2173.
(8) Chiang, I.; Brinson, B.; Huang, A.; Willis, P.; Bronikowski, M.; Margrave, J.; Smalley, R.; Hauge, R. *J. Phys. Chem. B* **2001**, *105*, 8297.
(9) Kuhlmann, U.; Jantoljak, H.; Pfander, N.; Bernier, P.; Journet, C.; Thomsen, C. *Chem. Phys. Lett.* **1998**, *294*, 237.
(10) Kastner, J.; Pichler, T.; Kuzmany, H.; Curran, S.; Blau, W.; Weldon, D.; Delamesiere, M.; Draper, S.; Zandbergen, H. *Chem. Phys. Lett.* **1994**, *221*, 53.
(11) Kuznetsova, A.; Mawhinney, D. B.; Naumenko, V.; Yates, J. T.; Liu, J.; Smalley, R. E. *Chem. Phys. Lett.* **2000**, *321*, 292.
(12) Mawhinney, D. B.; Naumenko, V.; Kuznetsova, A.; Yates, J. T. *J. Am. Chem. Soc.* **2000**, *122*, 2383.
(13) Nikiel, L.; Jagodzinski, P. *Carbon* **1993**, *31*, 1313.
(14) Kuznetsova, A.; Popova, I.; Yates, J. T.; Bronikowski, M. J.; Huffman, C. B.; Liu, J.; Smalley, R. E.; Hwu, H. H.; Chen, J. G. *J. Am. Chem. Soc.* **2001**, *123*, 10699.
(15) Kuznetsova, A.; Yates, J. T.; Simonyan, V. V.; Johnson, J. K.; Huffman, C. B.; Smalley, R. E. *J. Chem. Phys.* **2001**, *115*, 6691.
(16) Yim, W.; Byl, O.; Yates, J. T.; Johnson, J. K. *J. Chem. Phys.* **2004**, *120*, 5377.
(17) Williams, D. G.; Person, W. B.; Crawford, B. C. *J. Chem. Phys.* **1955**, *23*, 179.
(18) Yamada, H.; Person, W. B. *J. Chem. Phys.* **1964**, *41*, 2478.
(19) Borowiak-Palen, E.; Pichler, T.; Liu, X.; Knupfer, M.; Graff, A.; Jost, O.; Pompe, W.; Kalenczuk, R.; Fink, J. *Chem. Phys. Lett.* **2002**, *363*, 567.
(20) Liu, J.; Rinzler, A.; Dai, H.; Hafner, J.; Bradley, R. K.; Boul, P.; Lu, A.; Iverson, T.; Shelimov, K.; Huffman, C. B.; Rodriguez-Macias, F.; Shon, Y.; Lee, T. R.; Colbert, D.; Smalley, R. E. *Science* **1998**, *280*, 1253.
(21) Zhang, M.; Yudasaka, M.; Iijima, S. *J. Phys. Chem. B* **2003**, *108*, 149.
(22) Bachilo, S.; Strano, M.; Kittrell, C.; Hauge, R.; Smalley, R.; Weisman, R. B. *Science* **2002**, *298*, 2361.
(23) Strano, M.; Doorn, S.; Haroz, E.; Kittrell, C.; Hauge, R.; Smalley, R. *Nano Lett.* **2003**, *3*, 1091.
(24) Weisman, R. B.; Bachilo, S. *Nano Lett.* **2003**, *3*, 1235.
(25) Byl, O.; Kondratyuk, P.; Forth, S.; Fitzgerald, S.; Yates, J. T. *J. Am. Chem. Soc.* **2003**, *125*, 5889.
(26) Byl, O.; Kondratyuk, P.; Yates, J. T. *J. Phys. Chem. B* **2003**, *107*, 4277.
(27) Du, W.; Wilson, L.; Ripmeester, J.; Dutrisac, R.; Simard, B.; Denommee, S. *Nano Lett.* **2002**, *2*, 343.
(28) Williams, K. A.; Bhabendra, K. P.; Eklund, P. C.; Kostov, M. K.; Cole, M. W. *Phys. Rev. Lett.* **2002**, *88*, 165502.
(29) Narehood, D.; Kostov, M.; Eklund, P. C.; Cole, M. W.; Sokol, P. *Phys. Rev. B* **2002**, *65*, 233401.